Sparsity Weak Lensing Mass Reconstruction

ABSTRACT

1. INTRODUCTION

...

2. THE PROBLEM

2.1. Density Contrast to Shear

The lensing distortion κ at a position $\vec{x} = (\vec{\theta}, \chi_s)$ caused by the foreground inhomogeneous density distribution is

$$\kappa(\vec{\theta}, \chi_s) = \frac{3H_0^2 \Omega_M}{2c^2} \int_0^{\chi_s} d\chi_l \frac{\chi_l \chi_{sl}}{\chi_s} \frac{\delta(\chi_l \vec{\theta}, \chi_l)}{a(\chi_l)} \quad (1)$$

(Leonard et al. 2014). Substitute angular distance D with redshift z and we have

$$\kappa(\vec{\theta}, z_s) = \int_0^{z_s} dz_l \delta_c^{-1}(z_l, z_s) \delta(\vec{\theta}, z_l). \quad (2)$$

we term $\delta_c(z_l, z_s)$ as lensing critical density contrast and define it as

$$\delta_c^{-1}(z_l, z_s) = \begin{cases} \frac{3H_0 \Omega_M}{2c} \frac{\chi_l \chi_{sl}(1+z_l)}{\chi_s E(z_l)} & (z_s > z_l), \\ 0 & (z_s \leq z_l). \end{cases} \quad (3)$$

As reported in Kaiser & Squires (1993), the shear distortion is

$$\gamma(\vec{\theta}, z_s) = \int D(\vec{\theta} - \vec{\theta'}) \kappa(\vec{\theta'}, z_s) d^2\theta, \quad (4)$$

where

$$D(\vec{\theta}) = -\frac{1}{\pi}(\theta_1 - i\theta_2)^{-2},$$
$$\gamma(\vec{\theta}) = \gamma_1(\vec{\theta}) + i\gamma_2(\vec{\theta}). \quad (5)$$

Combine equation (2) with equation (4) and we have

$$\gamma(\vec{\theta}, z_s) = \int_0^{z_s} dz_l \frac{\delta_c(z_l, +\infty)}{\delta_c(z_l, z_s)} \int d^2\theta' D(\vec{\theta} - \vec{\theta'}) \frac{\delta(\vec{\theta'}, z_l)}{\delta_c(z_l, +\infty)}. \quad (6)$$

2.2. Photo-z Uncertainty

Since the redshifts of source galaxies are estimated with a limited number of photometric bands, the estimated redshift of a galaxy suffer from large uncertainty.
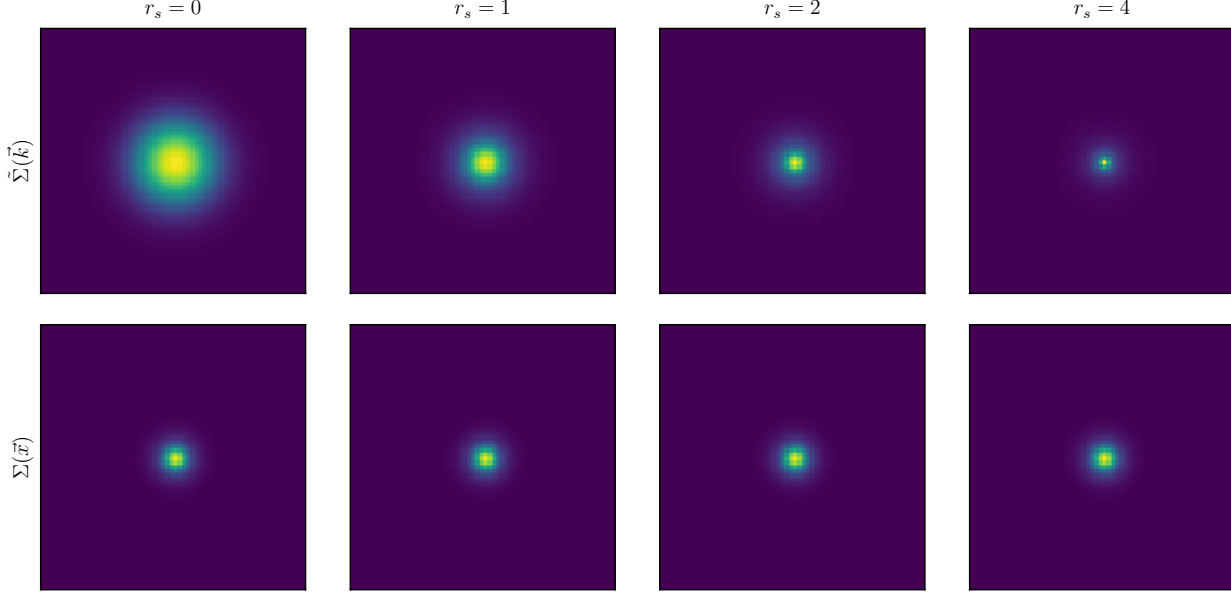
The probability distribution function (PDF) of a galaxies at position $(\vec{\theta}, z_s)$ is denoted as $\mathcal{P}(z|z_s)$. Note that, in order to simplify the future calculation, we assume the variation of the PDF across the transverse plane is small and neglect the dependency on the transverse position.

Taking the uncertainty of redshift into account, equation (6) changes to

$$\gamma(\vec{\theta}, z_s) = \int_0^{z_s} dz_l P(z_l, z_s) \gamma(\vec{\theta}, z_l, +\infty),$$
$$\gamma(\vec{\theta}, z_l, +\infty) = \int d^2\theta' Q(\vec{\theta} - \vec{\theta'}, z_l) \delta(\vec{\theta'}, z_l), \quad (7)$$

where $\gamma(\vec{\theta}, z_l, +\infty)$ represents shear signal at infinite redshift ($z_s = +\infty$) caused by density contrast at z_l, and $P(z_l, z_s)$ is the convolution kernel along line-of-sight and $Q(\vec{\theta}, \vec{\theta'}, z_l)$ is the convolution kernel along on the transverse plane. These kernels are defined as

$$P(z_l, z_s) = \int \frac{\delta_c(z_l, +\infty)}{\delta_c(z_l, z)} \mathcal{P}(z|z_s) dz,$$
$$Q(\vec{\theta}, \vec{\theta'}, z_l) = \frac{D(\vec{\theta} - \vec{\theta'})}{\delta_c(z_l, +\infty)}. \quad (8)$$

2.3. Smoothing

Since the observed galaxies have random irregular (unequally-spaced) distribution, it is necessary to smooth the shear signal in the observation. The smoothing is expressed as follows

$$\gamma_S(\vec{\theta}, z) = \frac{\sum_i W(\vec{\theta} - \vec{\theta}_i, z - z_i) e_i}{\sum_i W(\vec{\theta} - \vec{\theta}_i, z - z_i) R_i}, \quad (9)$$

where $W(\vec{\theta}, z)$ is a 3-D smoothing kernel. e_i, R_i, z_i and θ_i are the ellipticity, response, reshift, transverse position of the 'i-th' galaxy. $W(\vec{\theta}, z)$ can be decomposed into a transverse component $W_T(\vec{\theta})$ and a line-of-sight component $W_\times(z)$

$$W(\vec{\theta}, z) = W_T(\vec{\theta}) W_\times(z). \quad (10)$$

In this paper, we set

$$W_T(\vec{\theta}) = \frac{1}{2\pi\beta^2} \exp(-\frac{|\vec{\theta}|}{2\beta^2}),$$
$$W_\times(z) = \begin{cases} 1/\Delta z & (|z| < \Delta z/2), \\ 0 & else. \end{cases} \quad (11)$$

Figure 1. The NFW atom with different scale radius (r_s). The first row shows the NFW atoms in Fourier space and the second row shows the NFW atom in Real space.
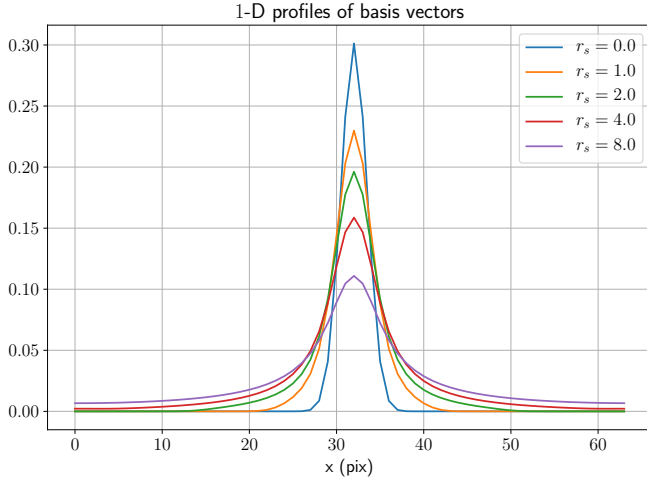

Figure 2. The 1-D slices of NFW atoms with different scale radius ($r_s = 0, 1, 2, 4, 8$).

With the assumption that the density of response R and the density of galaxy number vary slowly on the smoothing scale, the smoothed shear is

$$\gamma_S(\vec{\theta}_j, z_j) = \int d^2\theta_s dz_s W(\vec{\theta}_j - \vec{\theta}_s, z_j - z_s)\gamma(\vec{\theta}_s, z_s) \quad (12)$$

Substitute equation (7) into equation (12)

$$\gamma_S(\vec{\theta}_j, z_j) = \int_0^{z_j} dz_l P_S(z_l, z_j)\gamma_S(\vec{\theta}_j, z_l, +\infty),$$
$$\gamma_S(\vec{\theta}_j, z_l, +\infty) = \int d^2\theta' Q_S(\vec{\theta}_j, \vec{\theta'}, z_l)\delta(\vec{\theta'}, z_l), \quad (13)$$

and

$$P_S(z_l, z_j) = \int dz_s W_\times(z_j - z_s) \int \frac{\delta_c(z_l, +\infty)}{\delta_c(z_l, z)}\mathcal{P}(z|z_s)dz,$$
$$Q_S(\vec{\theta}, \vec{\theta'}, z_l) = \int d^2\theta'' W_T(\vec{\theta} - \vec{\theta''})\frac{D(\vec{\theta''} - \vec{\theta'})}{\delta_c(z_l, +\infty)}. \quad (14)$$

2.4. *Mask and Noise*

In real observations, the influence of mask and noise should also be taken into account. The final observed shear is

$$\gamma_o(\vec{\theta}, z) = M(\vec{\theta}, z)\gamma(\vec{\theta}, z) + \epsilon(\vec{\theta}, z), \quad (15)$$

where ϵ represents noise typically caused by random shape of intrinsic galaxies and such noise is modeled as white Gaussian noise. $M(\vec{\theta}, z_s)$ is the mask function.

We can write equation (15) into

$$\gamma_o = \mathbf{MPQ}\delta + \epsilon, \quad (16)$$

where $\mathbf{M}$, $\mathbf{P}$ and $\mathbf{Q}$ represent the functional operators M, P and Q, respectively.

3. THE METHOD

3.1. *Dictionary*

Since many N-body simulations have shown the dark matter to be largely distributed in halos connected by filaments, we assume that the density contrast field can

be decomposed into multi-scaled NFW halo (Navarro et al. 1997) and point mass at different positions

$$\delta(\vec{x}) = \sum_{s=0}^{N_s} \int d^3x' \phi_s(\vec{x} - \vec{x}')\alpha_s(\vec{x'}) \qquad (17)$$

where ϕ_0 is 3-D Dirac delta function representing point mass

$$\phi_0(\vec{x}) = \delta_D(\theta_1)\delta_D(\theta_2)\delta_D(z). \qquad (18)$$

Since the scale of halo is much less than the reachable redshift resolution, we neglect the depth of halo on the line-of-sight direction as suggested by (Leonard et al. 2014). On the transverse plane, the NFW atom is modeled with the surface density profile of NFW halo with scale θ_s and truncation radius $c\theta_s$ (Takada & Jain 2003), where c is generally known as concentration of NFW halo. Whereas, the NFW atom is modeled with Dirac delta function on the line-of-sight direction

$$\phi_s(\vec{x}) = \frac{f}{2\pi\theta_s^2}F(|\vec{\theta}|/\theta_s)\delta_D(z),$$
$$(s = 1..N_s) \qquad (19)$$

where

$$F(x) = \begin{cases} -\frac{\sqrt{c^2-x^2}}{(1-x^2)(1+c)} + \frac{1}{(1-x^2)^{3/2}}\text{arccosh}(\frac{x^2+c}{x(1+c)}) & (x < 1), \\ \frac{\sqrt{c^2-1}}{3(1+c)}(1 + \frac{1}{c+1}) & (x = 1), \\ -\frac{\sqrt{c^2-x^2}}{(1-x^2)(1+c)} + \frac{1}{(x^2-1)^{3/2}}\arccos(\frac{x^2+c}{x(1+c)}) & (1 < x \leq c), \\ 0 & (x > c). \end{cases} \qquad (20)$$

and $f = 1/[\ln(1+c) - c/(1+c)]$.

α_s is the corresponding decomposition coefficient of the density contrast field onto our basis atom. The total coefficients set is denoted as $\alpha = \begin{pmatrix} \alpha_0 \\ \alpha_1 \\ ... \\ \alpha_{N_s} \end{pmatrix}$, and the total dictionary is $\Phi = \left(\phi_0, \phi_1, ..., \phi_{N_s}\right)$.

We pixelize the parameter space into a $N_\theta \times N_\theta \times N_l$ grid. N_θ is the number of pixels on the two dimensions of the transverse plane and N_l is the number of pixels on the line-of-sight direction for the lenses. Similarly, γ_o is pixelized onto a $N_\theta \times N_\theta \times N_s$ grid, where N_s is the number of pixel on the line-of-sight direction for the sources. The pixel size for the two dimensions on the transverse plane is denoted as $\Delta\theta$ and the pixel size for the line-of-sight direction is denoted as Δz. Equation (16) changes to

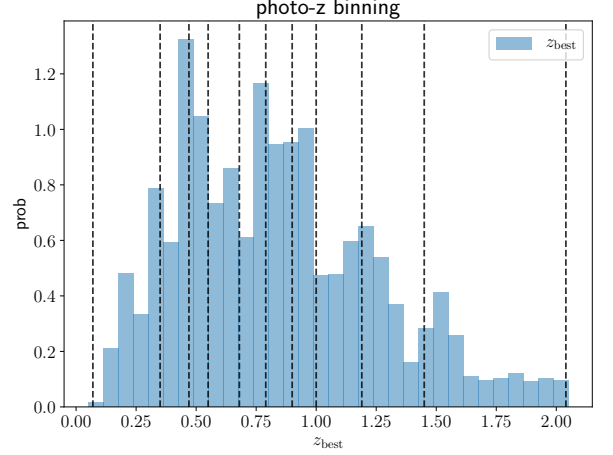$$\gamma = \mathbf{MPQ\Phi}\alpha + \epsilon. \qquad (21)$$

Figure 3. The source galaxies are binned into 10 redshift bins according to their mlz best photo-z estimation. The blue histogram is the number distribution of the best photo-z estimation. The vertical dashed lines are the bounds of bins. The galaxies are evenly distributed in each bins.

3.2. *Loss Function with Constrains*

The loss function is defined as

$$L = \|\gamma - \mathbf{MPQ\Phi}\alpha\|_2^2 + \lambda\|\alpha\|_1^1 + \tau\text{TSV}(\alpha_0), \qquad (22)$$

where $\|\gamma - \mathbf{MPQ\Phi}\alpha\|_2^2$ is the normal chi-square, $\|\alpha^{N,P}\|_1^1$ is the sparsity constrain, and $\text{TSV}(\alpha^P)$ is the Total Squared Variation (TSV) constrain. $\|\bullet\|_1$ and $\|\bullet\|_2$ represent l_1 norm and l_2 norm, respectively. The TSV operator is defined as

$$\begin{aligned} \text{TSV}(\alpha_0) = \sum_{ijk} &\{(\alpha_0[i,j,k] - \alpha_0[i+1,j,k])^2 \\ &+ (\alpha_0[i,j,k] - \alpha_0[i,j+1,k])^2 \\ &+ (\alpha_0[i,j,k] - \alpha_0[i,j,k+1])^2\}, \end{aligned} \qquad (23)$$

where $i = 1..N_\theta$, $j = 1..N_\theta$, are the pixel indexes for the two dimensions on the transverse plane, $k = 1..N_l$ is the pixel index on the line-of-sight direction.

We define

$$\begin{aligned} f(\alpha) &= \|\gamma - \mathbf{MPQ\Phi}\alpha\|_2^2 + \tau\text{TSV}(\alpha^P) \\ &= \sum_{lm} A_{lm}\alpha_l\alpha_m + \sum_l B_l\alpha_l + C, \end{aligned} \qquad (24)$$

where l, m go over the indexes of (i, j, k, s).

3.3. *FISTA*

The basic FISTA algorithms is

$$X_m^{(n+1)} = \text{ST}_\lambda(\alpha_m - \frac{\mu}{2A_{mm}}\frac{\partial f}{\partial \alpha_m})|_{\alpha_m^{(n)}}, \qquad (25)$$
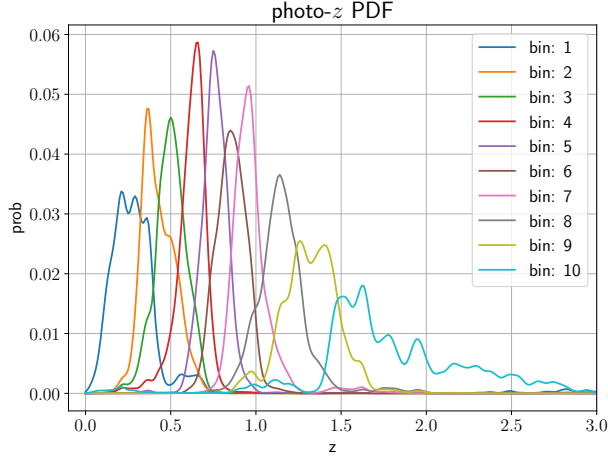
Figure 4. The PDF of photo-z error for 10 source redshift bins.
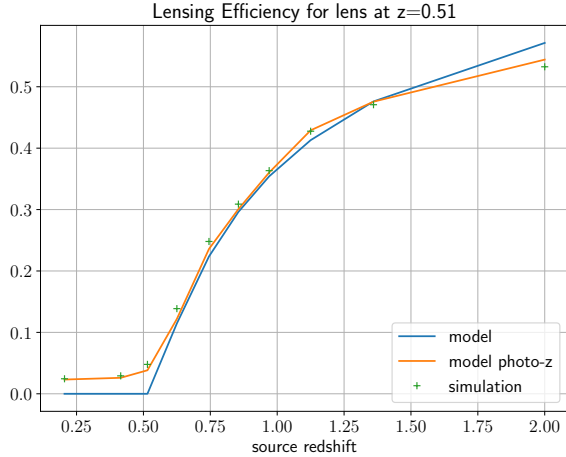

Figure 5. The blue line shows the normalized lensing efficiency for lens bin at $z_l = 0.51$. The orange line is the normalized lensing efficiency while taking into account the photo-z uncertainty.

where

$$\mathrm{ST}_\lambda(x) = \mathrm{sign}(x) \max(|x| - \lambda, 0) \qquad (26)$$

is the soft thresholding function.

$$
\begin{aligned}
t^{(n+1)} &= \frac{1 + \sqrt{1 + 4(t^{(n)})^2}}{2}, \\
\alpha_m^{(n+1)} &= X_m^{(n+1)} + \left[\frac{t^{(n)} - 1}{t^{(n+1)}}(X_m^{(n+1)} - X_m^{(n)})\right],
\end{aligned}
\qquad (27)
$$

with $t^{(0)} = 1$ and $X^{(0)} = \alpha^{(0)}$.

4. HSC-LIKE SIMULATION

4.1. *Shear Measurement Error*

4.2. *Photo-z Error*

5. RESULTS

6. SUMMARY

REFERENCES

Kaiser, N., & Squires, G. 1993, ApJ, 404, 441, doi: 10.1086/172297

Leonard, A., Lanusse, F., & Starck, J.-L. 2014, MNRAS, 440, 1281, doi: 10.1093/mnras/stu273

Navarro, J. F., Frenk, C. S., & White, S. D. M. 1997, ApJ, 490, 493, doi: 10.1086/304888

Takada, M., & Jain, B. 2003, MNRAS, 340, 580, doi: 10.1046/j.1365-8711.2003.06321.x

APPENDIX

A. GENERAL LINEAR LASSO

Note that the loss function defined in equation (22) into

$$L(\alpha) = f(\alpha) + \lambda \|\alpha\|_1^1, \tag{A1}$$

where

$$f(\vec{\alpha}) = \vec{\alpha}^T \mathbf{A} \vec{\alpha} + \vec{B} \cdot \vec{\alpha} + C. \tag{A2}$$

Using Einstein notation, we have

$$L(\alpha_i) = A_{ij}\alpha_i\alpha_j + B_i\alpha_i + C + \lambda_i|\alpha_i|. \tag{A3}$$

Set the initial parameter vector is $\vec{\alpha}^{(0)}$. We focus on one specific parameter with index μ and fix other parameters with indexes $i \neq \mu$

$$L(\alpha_\mu|\alpha_{i\neq\mu}^{(0)}) = A_{\mu\mu}\alpha_\mu^2 + (A_{i\mu}\alpha_i^{(0)} + A_{\mu i}\alpha_i^{(0)} + B_\mu)\alpha_\mu + \lambda_\mu|\alpha_\mu| + B_i\alpha_i^{(0)} + \lambda_i\left|\alpha_i^{(0)}\right| + C \tag{A4}$$

reach its minimum at $\mathrm{ST}_\lambda(\alpha_\mu - \frac{\partial_\mu f(\alpha_\mu|\alpha_{i\neq\mu}^{(0)})}{2A_{\mu\mu}})|_{\alpha_\mu^{(0)}}$, where $\mathrm{ST}_\lambda(x) = \mathrm{sign}(x)\max(|x| - \lambda, 0)$ is the soft thresholding function. Then the parameter can be updated

$$\alpha_\mu^{(1)} \leftarrow \mathrm{ST}_\lambda(\alpha_\mu - \frac{\partial_\mu f(\alpha_\mu|\alpha_{i\neq\mu}^{(0)})}{2A_{\mu\mu}})|_{\alpha_\mu^{(0)}}. \tag{A5}$$

Other parameters are subsequently updated in the same way. The minimum of the loss function can be reached by iterating the parameter update.